Sci. Rep. Kanazawa Univ.,
Vol. 22, No. 1, pp. 31-43
June 1977

Radiochemical Studies of Deep-Sea Manganese Nodules

Takashi NAKANISHI, Mikiko OOHASHI*, Michiko HIGASHI**
and Masanobu SAKANOUE

Radiochemical Laboratory, Department of Chemistry,
Faculty of Science, Kanazawa University

(Received April 26, 1977)

Abstract Isotopic composition of uranium, thorium and protactinium was determined radiochemically in a manganese nodule dredged from the Suiko Seamount, North Pacific Ocean. The elemental distribution in this manganese nodule was also studied by electron microprobe X-ray analysis, alpha track, fission track, and activation autoradiographic methods. The excess ^{230}Th and ^{231}Pa activities were found to decrease with depth in the crust of few mm thick of the manganese nodule from Suiko Seamount. But, in the inner part of this nodule, deficiencies of ^{230}Th and ^{231}Pa were found. A slow growth of the crust after a comparatively rapid formation of the inner part was suggested from these results. A comparative study on the elemental distribution in a manganese nodule dredged from the Central Equatorial Pacific Ocean showed a somewhat different pattern of elemental distribution from the Suiko nodule.

1. Introduction

The genetic origin of manganese nodules has been a subject of considerable interest for many investigators, and intensively studied through the chemical and mineralogical aspects[1)-3)]. And its growth rate has been determined since the advent of radiometric dating techniques. Earlier papers[4)-10)] have reported slow accumulation rates of something like a few mm per million years. However, in reference to the comparatively rapid accumulation rate of a few mm per thousand years of deep sea sediment, it is very difficult to account that large manganese nodules stay on the surface of sea floor. It may be said that the formation of oceanic manganese nodules is still an open question.

In this paper, the contents of ^{238}U (half life: 4.51×10^{9} years), ^{234}U (2.47×10^{5} years), ^{232}Th (1.39×10^{10} years), ^{230}Th (7.5×10^{4} years) and ^{231}Pa (3.25×10^{4} years) were determined radiochemically on a large Suiko manganese nodule from its surface to the core. Furthermore, the distribution patterns of some chemical elements and α-emitting

* the new surname and present address: MUKAI, 2-9, Shin-ikecho, Chikusa-ku, Nagoya.
** the new surname and present address: ENDOU, 2-14-34, Chu-ou, Yamato.

nuclides in the surface layer of about 3 mm thick of this nodule were studied by applying electron microprobe X-ray analysis (XMA), activation autoradiographic technique (activography)[11], fission track and alpha track methods. A small manganese nodule from the Central Equatorial Pacific was also examined by fission track and activographic methods.

2. Materials and methods

A large manganese nodule sample subjected to this work was dredged during the KH-68-3 cruise of the Research Vessel Hakuho-maru in August, 1968, from the Suiko Seamount (44° 37′ N, 170° 18′E, St.-9-7, water depth 1365-1820 m) belonging to the Emperor Seamounts of North Pacific Ocean. Some silicic plutonic rocks coated with ferromanganese oxide of less than 1 mm thick were found in the dredged samples from this station[12]. A few olivine basalts covered with ferromanganese oxide of about 20-30 mm thick were also dredged from other station belonging to the Suiko Seamount, and the K-Ar ages of volcanic rocks from this seamount were about 21-42 million years[13]

This large nodule sample was cut into two parts as shown in Plate I. The fine concentric banding produces annular rings and there are no appreciable inclusions in the core. For the radiometric work, arc-shaped sections were scraped with a dental drill from the surface to the core along the line indicated in Plate I. The thickness of each analyzed sections was measured with a calipers with an error of ± 0.1 mm or less and was as follows: 0.1-1.5 mm thick for the samples from the surface to 4 mm depth, 3-6 mm thick for the inner layer samples and 13 mm in diameter for the core. Each scraped samples was weighed after dried overnight at 110 °C and then digested with about 50 ml of 8 M HCl containing 0.01 M HF and about 1 ml of 30% H_2O_2 solution. The sample solution spiked with ^{232}U, ^{234}Th and ^{233}Pa tracers was boiled for one hour to attain isotopic exchange equilibrium and then diluted with water. The insoluble materials were removed by centrifugation and their amounts were from 2 to 5 % of the nodule material on a dry weight basis. Radiochemical separation of uranium, thorium and protactinium from the sample solution was carried out by means of anion-exchange method and the final purification of uranium and protactinium was carried out by solvent extraction with TnOA and DIBK, respectively, and that of thorium by cation-exchange resin[14]. After electrodeposition of the purified uranium, thorium and protactinium fractions on stainless steel plates, alpha spectrometry was carried out by a double-gridded ionization chamber connected to a 100 channel pulse height analyzer. The counting efficiency was 46.7 ± 1.2 %.

To study the depth distribution of some chemical elements and alpha-particle emitters in the crust, a broken piece of the crust of the Suiko manganese nodule (0-3 mm section) was fixed in epoxy resin and the cross section was polished. A cellulose nitrate film was placed in a close contact to the polished section for about three months and a mapping of alpha activity was obtained by observing alpha tracks in this film.

For the uranium mapping, fission track technique was applied by using a muscovite as a track detector. The neutron irradiation was performed with a thermal flux of 4×10^{11} n/cm^2/sec[15] for 300 min in a TRIGA Mark-II nuclear reactor. A pressed homogenized powder sample of manganese nodule with a known uranium content was also irradiated as a reference standard. By applying autoradiographic technique (activography) to the neutron irradiated sample, the fine distribution of manganese and cobalt in the polished section could be known by its induced radioactivities. The nuclides responsible for the respective autoradiographic image was identified by gamma-ray spectrometry. The fine distribution patterns of manganese, iron, cobalt and nickel were also studied by an electron microprobe X-ray analyzer (XMA).

Another sample of manganese nodule was obtained from south of the Mid-Pacific Seamounts of the Central Equatorial Pacific Ocean (between 9°16′7″N, 179°19′6″W and 9°16′3″N, 179°20′5″W, St. 34, water depth 5940 m). The dredging of this nodule was made in January, 1968, during the KH-67-5 cruise of the Research Vessel Hakuho-maru. This manganese nodule was of a form of agglomeration of several concretions, having a tabular shape on the whole. A flat sample section was sliced from a small concretion containing phosphate mineral in its core and was subjected to the fission track and activographic studies.

3. Results and discussion

3.1. *Uranium, thorium and protactinium isotopes in the Suiko nodule*

The results on the contents of ^{238}U, ^{234}U, ^{232}Th, ^{230}Th and ^{231}Pa in the Suiko

Table 1 U, Th and Pa isotopes in the Suiko manganese nodule (specific radioactivity on a dry weight basis).

depth (cm)	^{238}U * (dpm/g)	^{234}U (dpm/g)	^{235}U ** (dpm/g)	^{232}Th * (dpm/g)	^{230}Th (dpm/g)	^{231}Pa (dpm/g)
0 - 0.01	14.1 ± 2.0	14.4 ± 2.0	0.65 ± 0.09	17.8 ± 1.8	145 ± 4	18.3 ± 1.5
0.01 - 0.05	15.3 ± 1.4	16.6 ± 1.5	0.71 ± 0.07	17.6 ± 0.7	101 ± 3	10.7 ± 0.9
0.05 - 0.11	15.3 ± 2.1	16.6 ± 2.3	0.71 ± 0.10	17.9 ± 0.9	68.7 ± 3.4	5.49 ± 1.37
0.11 - 0.25	14.2 ± 0.7	15.4 ± 0.8	0.66 ± 0.04	18.4 ± 0.7	41.9 ± 1.3	1.27 ± 0.10
0.25 - 0.40	15.9 ± 0.6	14.4 ± 0.6	0.74 ± 0.03	15.0 ± 0.6	18.9 ± 0.8	1.44 ± 0.14
0.4 - 0.7	16.7 ± 1.1	18.6 ± 1.2	0.77 ± 0.05	7.64 ± 0.48	14.7 ± 0.8	1.21 ± 0.30
0.7 - 1.0	16.8 ± 0.8	16.9 ± 0.8	0.78 ± 0.04	6.13 ± 0.30	16.1 ± 0.6	1.23 ± 0.39
1.0 - 1.3	13.7 ± 0.9	15.0 ± 1.0	0.64 ± 0.04	8.34 ± 0.29	12.8 ± 0.5	1.40 ± 0.12
1.3 - 1.7	13.2 ± 0.6	13.9 ± 0.7	0.61 ± 0.03	8.26 ± 0.30	15.2 ± 0.5	1.20 ± 0.09
1.7 - 2.3	15.9 ± 0.7	15.3 ± 0.7	0.73 ± 0.03	8.43 ± 0.28	13.4 ± 0.4	2.27 ± 0.12
2.3 - 2.8	13.8 ± 0.9	13.9 ± 0.9	0.64 ± 0.04	8.91 ± 0.29	14.9 ± 0.5	1.03 ± 0.08
2.8 - 3.3	15.9 ± 0.9	16.3 ± 0.9	0.74 ± 0.04	8.76 ± 0.30	14.7 ± 0.5	0.53 ± 0.06
3.8 - 4.3	12.6 ± 0.7	13.6 ± 0.7	0.59 ± 0.03	10.7 ± 0.6	11.5 ± 0.6	0.52 ± 0.06
4.8 - 5.2	7.36± 0.47	7.38± 0.47	0.34 ± 0.02	6.56 ± 0.22	5.30 ± 0.17	0.28 ± 0.04
5.2 - 5.7	6.25± 0.59	6.35± 0.60	0.29 ± 0.03	6.11 ± 0.23	5.49 ± 0.21	0.28 ± 0.05
5.7 - 7.0	7.01± 0.40	7.21± 0.41	0.33 ± 0.02	6.17 ± 0.22	6.40 ± 0.22	0.33 ± 0.07

* 1 μg ^{238}U = 0.739 dpm
1 μg ^{232}Th = 0.246 dpm

** calculated on the basis of $A^{235}_{U} = A^{238}_{U} / 21.58$

manganese nodule are given in table 1 on a dry weight basis. The uncertainties indicated were due to the counting statistics ($\pm$ 1σ). The concentration of ^{235}U was calculated from that of ^{238}U using the natural abundance value of 0.72 % for ^{235}U.

Concentration of uranium and thorium

In fig. 1, the uranium and thorium data on the Suiko nodule are plotted against the depth from the surface. The concentration of uranium in this manganese module was about 20 ppm in the sections from 0 to 4.3 cm and about 10 ppm in the sections from 4.8 to 7.0 cm. The concentration of thorium in the surface crust was about 75 ppm, and decreased to about 30 ppm at 1 cm, followed by the slight increase to about 45 ppm between 1–4 cm and the decrease to about 25 ppm at the 5–7 cm interval. These values of uranium and thorium were higher than the reported values for another manganese nodules from the same dredge station[16].

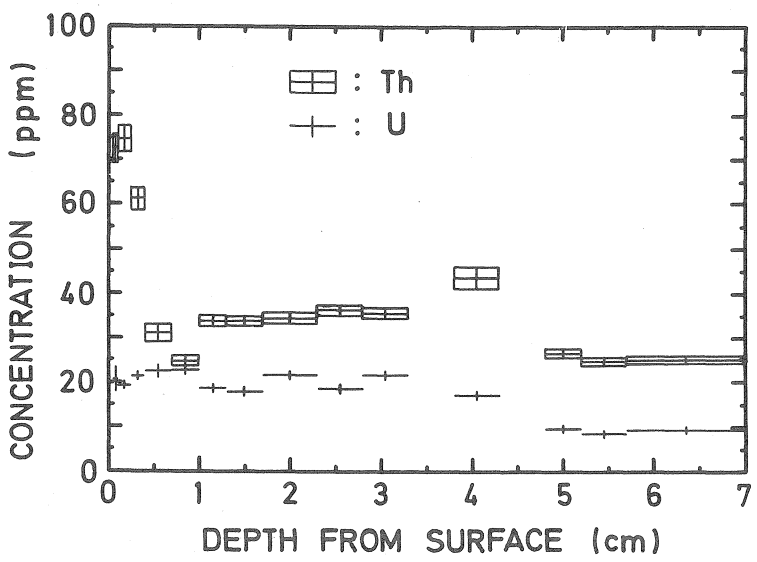

Fig. 1 Depth distribution of uranium and thorium in the Suiko manganese nodule.

It is interesting to compare the concentrations of uranium and thorium in the manganese nodule with those of 1.11–2.47 ppm uranium and 5.95–11.3 ppm thorium in the pelagic sediments[17] from almost the same area of the Central North Pacific (43°24′ N, 178°52′W ; 45°27′N, 179°15′W ; 47°19′N, 179°39′W). The weight ratio of thorium to uranium varied from about 1 to about 4 in the Suiko nodule as shown in fig. 2. These values of the ratio are, however, distinctly lower than those of 4.4–7.9 for the pelagic sediments[17]. This fact may be due in part to the difference of the sources of uranium and thorium in manganese nodule and pelagic sediment, and to the greater abundance of detrital materials in the pelagic sediment.

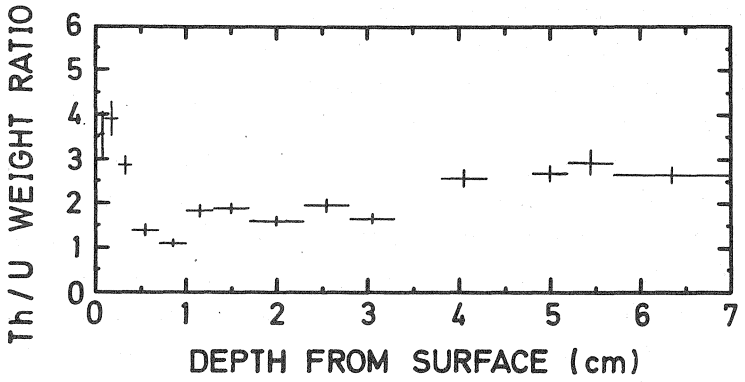

Fig. 2 Weight ratios of thorium to uranium in the Suiko manganese nodule.

The concentration of uranium, thorium and the Th/U ratio seems to vary somewhat systematically in the fairly large manganese nodule studied. This variation seems to reflect unsteady condition of formation for this manganese nodule, and the higher concentration of thorium in the crust may be due to a slow formation of the crust compared with the growth rate of the inner part (see the discussion below).

$^{230}Th/^{234}U$ and $^{231}Pa/^{235}U$ activity ratios

Excess ^{230}Th and ^{231}Pa calculated from the measured values (table 1) decreased

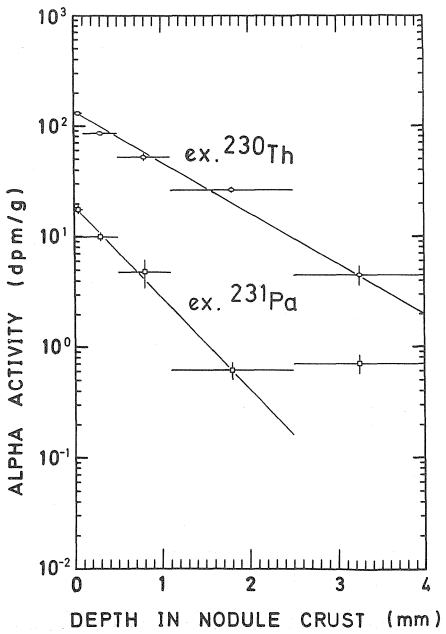

Fig. 3 Specific alpha radioactivities of excess ^{230}Th and ^{231}Pa as a function of depth in the crust of the Suiko manganese nodule.

with depth in the crust of the Suiko nodule as shown in fig. 3. The accumulation rate of this crust can be estimated to be (9±2) mm/10^6 years from excess ^{230}Th and (11±4) mm/10^6 years from excess ^{231}Pa by assuming the constant precipitation of ^{230}Th and ^{231}Pa. The uncertainties are due to counting statistics and width of each analyzed section. The activity ratio of excess ^{230}Th to excess ^{231}Pa in the 0–0.1 mm section was 7.4±0.7, and less than the production ratio of 10.8 of these two nuclides from the precursor uranium isotopes dissolved in the sea water. This indicates preferential deposition of ^{231}Pa during the formation of manganese nodule as mentioned by Sackett[18]. The ^{230}Th/^{232}Th ratio in the 0–0.1 mm section was about 8, and lower than that of about 15 in the surface of pelagic sediment from the North Pacific[18]. This may be due to the preferential precipitation of ^{230}Th on the pelagic sediment.

The activity ratios of ^{230}Th/^{234}U, ^{231}Pa/^{235}U and ^{234}U/^{238}U are plotted against depth in figs. 4, 5 and 6. It becomes fairly difficult to detect excess ^{230}Th in the sections deeper than 5 mm from the surface. At the positions between 2.8–5.7 cm, ^{230}Th is rather deficient from the equilibrium value, and in 4.8–5.2 cm section the deficiency is obvious with 95.5 % confidence. The deficiency of ^{231}Pa from the equilibrium is obvious in the 2.8–3.3 cm section with 95.5 % confidence, although the excess activity was found even in the 2.3–2.8 cm section. Assuming that an ideal closed system was held, the maximum age may be determined by using the growth of ^{230}Th and ^{231}Pa from uranium isotopes for the sections where the ^{230}Th/^{234}U or ^{231}Pa/^{235}U activity ratio is lower than the equilibrium value[19]. Using the relation of $t_{max}\ (R) = -\frac{1}{\lambda R} \cdot \ln\left(1-\frac{R}{U}\right)$, where R is

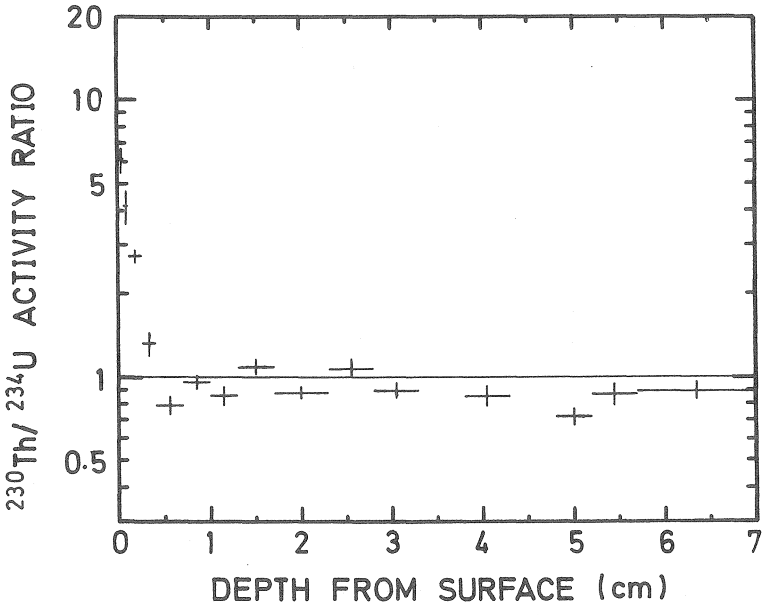

Fig. 4 Depth distribution of ^{230}Th/^{234}U activity ratio in the Suiko manganese nodule.

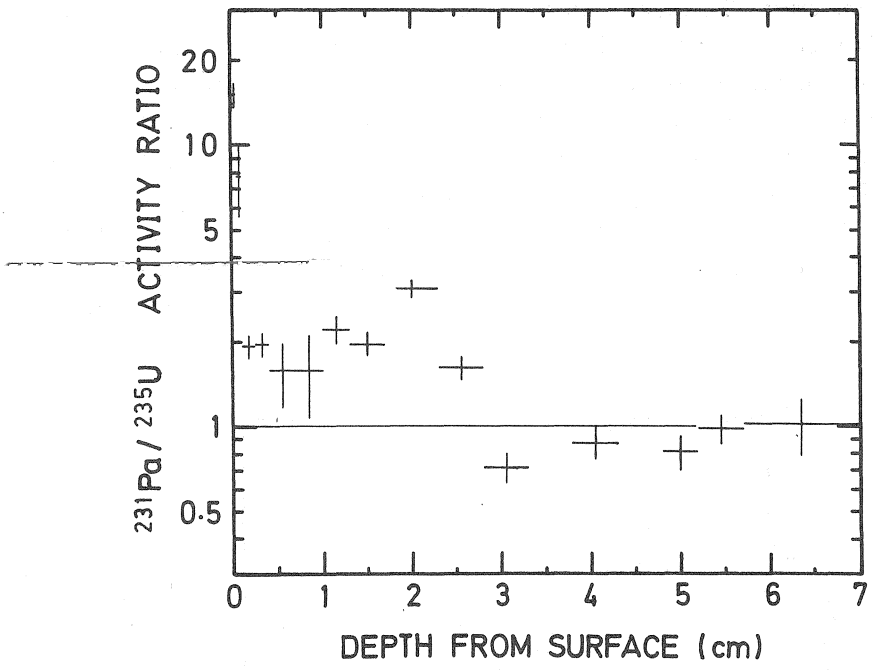

Fig. 5 Depth distribution of ^{231}Pa/^{235}U activity ratio in the Suiko manganese nodule.

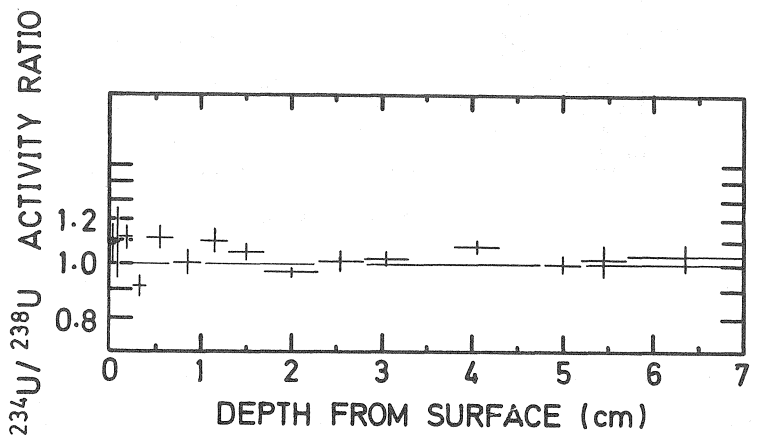

Fig. 6 Depth distribution of ^{234}U/^{238}U activity ratio in the Suiko manganese nodule.

^{230}Th or ^{231}Pa, about $(0.3\text{–}1.1)\times 10^5$ years for the 2.8–3.3 cm section was obtained from the ^{231}Pa/^{235}U value of 0.7 ± 0.2 ($\pm 2\sigma$), and about $(0.9\text{–}1.7)\times 10^5$ years for the 4.8–5.3 cm section from the ^{230}Th/^{234}U value of 0.7 ± 0.1 ($\pm 2\sigma$). These maximum ages are younger than those estimated from the accumulation rates based on the decrease of excess ^{230}Th

and ^{231}Pa in the crust. This fact probably means a slow formation of the crust after a comparatively rapid formation of the bulk of the inner part. If the surface crust were formed slowly in the same manner as that of ferromanganese coating on plutonic rocks dredged together with this manganese nodule, the thickness formed by slow process may be 1 mm at most. Fig. 7 explains the relation between the above mentioned $^{230}Th/^{234}U$ and $^{231}Pa/^{235}U$ maximum age and the 1 mm thickness of slow formation after this rapid process. This process may also be supported by the high concentration of thorium isotopes and protactinium in the crust, although all radiochemical patterns in the inner layers can not be explained without the consideration of a migration or a diffusion of elements.

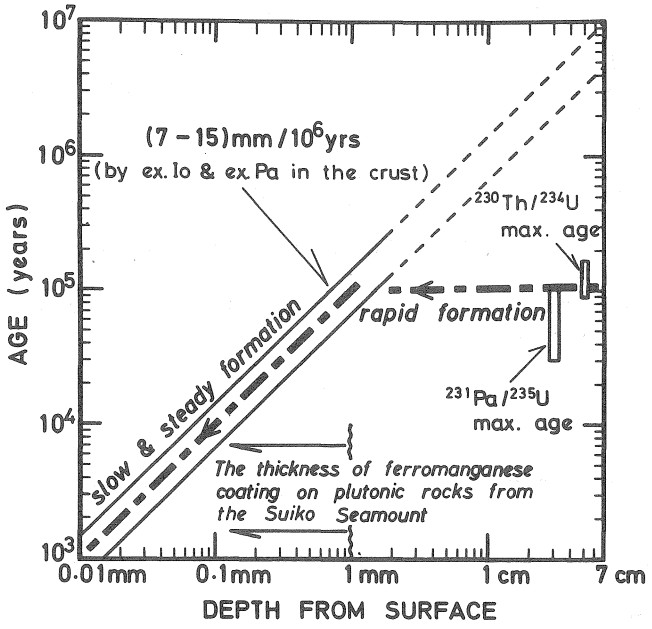

Fig. 7 Schematic illustration on the formation process of the Suiko manganese nodule (Io=^{230}Th, Pa=^{231}Pa).

The $^{234}U/^{238}U$ ratio varied in a range from 1.1 to 0.9 in the 0–1.7 cm, but it was about the unity in the 1.7–7 cm sections. Experimental values of less than 1.00 may be attributed to post-depositional migration of ^{234}U, though the excess ^{234}U near the surface may reflect the younger age than 10^6 years.

3.2. *The fine distribution of some chemical elements in the crust of the Suiko nodule*

The detailed studies on the fine distribution of chemical elements and alpha radioactivities were made for the crust of the Suiko manganese nodule, where a high concentration of ^{232}Th, ^{230}Th and ^{231}Pa was observed. Plate II is the summary of these studies to compare the results of XMA, fission track and alpha track analyses along

with a reflecting photomicrograph of a polished cross section of the crust.

Iron, cobalt, manganese and nickel are shown to distribute considerably inhomogeneously within the scanned line of 2 mm and less from the surface. The inter-elemental associations among these elements seem to exist in correlation with the concentric banding. The activography of cobalt showed a reasonable agreement in the distribution pattern with the result of the XMA analysis. These distribution patterns also indicate the differential accumulation of these elements.

The distribution of uranium measured by fission track technique indicates a depth variation between 15–20 ppm, but the correlation with the fine concentric banding is not clear.

In the 0–0.5 mm layer, a high alpha particle track density was observed relative to that at the 1–3 mm layer, and may be due to the excess ^{230}Th. In the extreme surface, a cluster of alpha track was observed (@ in Plate II), and this may indicate inhomogeneous precipitation of ^{230}Th in the form of radiocolloid on the surface of manganese nodule. A large track cluster of about 0.5 mm in diameter was also confirmed at the position of about 3 mm from the surface (© in Plate II) by two independent observations with different cellulose nitrate films for the same surface, in spite of uniform distribution of uranium in this region by fission track method. If a large number of such clusters exist sporadically in a sample, the excess ^{230}Th method for dating of manganese nodule may be invalidated in some cases.

3.3. *The distribution of U, Mn and Co in the Equatorial Pacific manganese nodule*

The result of uranium mapping of the Equatorial Pacific manganese nodule examined by fission track technique is given in Plate III, together with activographic images of manganese and cobalt. This nodule consisted of alternative bands of different light reflection (see the photo at upper left in Plate III). While the less reflective bands contain greater amounts of detrital silicates and manganese than do the reflective ones, the more reflective bands contain greater amounts of cobalt and consist of granules of about 0.2 mm in diameter. The distribution of uranium was found to be similar to that of cobalt, though the concentration of uranium was about the half of the Suiko manganese nodule. Such type of structure was not observed in the Suiko manganese nodule, and this is probably attributed to the difference of the formation mechanism between the Suiko manganese nodule and the one from Equatorial Pacific.

Acknowledgments

The authors thank Drs. K. Kobayashi and K. Kitazawa of the Ocean Research Institute, University of Tokyo, for providing manganese nodules, Dr. S. Banno of the Faculty of Science, Kanazawa University, for his help in XMA analysis, and Dr. H. Higuchi of the Institute for Atomic Energy, Rikkyo University, for his support in neutron irradiation. We are also indebted to Dr. K. Sakamoto of our laboratory who critically read the manusucript.

References

1) E. Bonatti and Y. R. Nayudu, The origin of manganese nodules on the ocean floor, Am. J. Sci., 263 (1965) 17.
2) K. Bostrom, The problem of excess manganese in pelagic sediments, Researches in Geochemistry, vol. 2, P. H. Abelson ed., John Wiley & Sons, Inc., New York, (1976) 421.
3) J. S. Tooms, S. P. Summerhayes and D. S. Cronan, Geochemistry of marine phosphate and manganese deposits, Oceanogr. Mar. Biol. Ann. Rev., 7 (1969) 49.
4) M. L. Bender, T. L. Ku and W. S. Broecker, Manganese nodule: their evolution, Science, 151 (1966) 325.
5) T. L. Ku and W. S. Broecker, Uranium, thorium, and protactinium in a manganese nodule, Earth Planet. Sci. Letters, 2 (1967) 317.
6) S. S. Barnes and J. R. Dymond, Rates of accumulation of ferro-manganese nodules, Nature, 213 (1967) 1218.
7) B. L. K. Somayajulu, Beryllium-10 in a manganese nodule, Science, 156 (1967) 1219.
8) T. L. Ku and W. S. Broecker, Radiochemical studies on manganese nodules of deep sea origin, Deep-Sea Res., 16 (1969) 625.
9) B. L. K. Somayajulu, G. R. Heath, T. C. Moore, Jr. and D. S. Cronan, Rates of accumulation of manganese nodules and associated sediment from the equatorial Pacific, Geochim. Cosmochim. Acta, 35 (1971) 621.
10) J. L. Bada, The dating of fossile bones using the racemization of isoleucine, Earth Planet. Sci. Letters, 15 (1972) 223.
11) M. Sakanoue, M. Yoshioka, T. Nakanishi and T. Takagi, Studies on the distribution of chemical elements in geochemical samples by an activation autoradiographic method, Intern. J. Appl. Rad. Isotopes, 22 (1971) 177.
12) H. Aoki and H. Hirata, Rocks on ocean floor-Suiko Seamount-(in Japanese), Marine Sciences, 3 (1971) 852.
13) M. Ozima, I. Kaneoka and S. Aramaki, K-Ar ages of submarine basalts dredged from seamounts in the western Pacific area and discussion of oceanic crust, Earth Planet. Sci. Letters, 8 (1970) 237.
14) M. Sakanoue, K. Konishi and K. Komura, Stepwise determinations of thorium, protactinium and uranium isotopes and their application for geochronological studies, IAEA Symposium on Radioactive Dating and Methods of Low-Level Counting, IAEA STI/PUB/152 (1967) 313.
15) M. Sakanoue and T. Nakanishi, Measurement of neutron flux in nuclear reactor by means of fission track method (in Japanese), J. At. Energy Soc. Japan, 11 (1969) 332.
16) A. Okada and M. Shima, Study on the manganese nodule (in Japanese), J. Oceanographical Soc. Japan, 26 (1970) 151.
17) T. L. Ku, W. S. Broecker and N. Opdyke, Comparison of sedimentation rates measured by paleomagnetic and Io methods of age determination, Earth Planet. Sci. Letters, 4 (1968) 1.
18) W. M. Sackett, Manganese nodule: thorium-230: Protactinium-231 ratios, Science, 154 (1966) 646.
19) V. V. Cherdyntsev, N. B. Kadyrov and N. V. Novichkova, Origin of the Pacific manganese nodules, based on the content of radioisotopes, Gekhimiya, No. 3 (1971) 339.

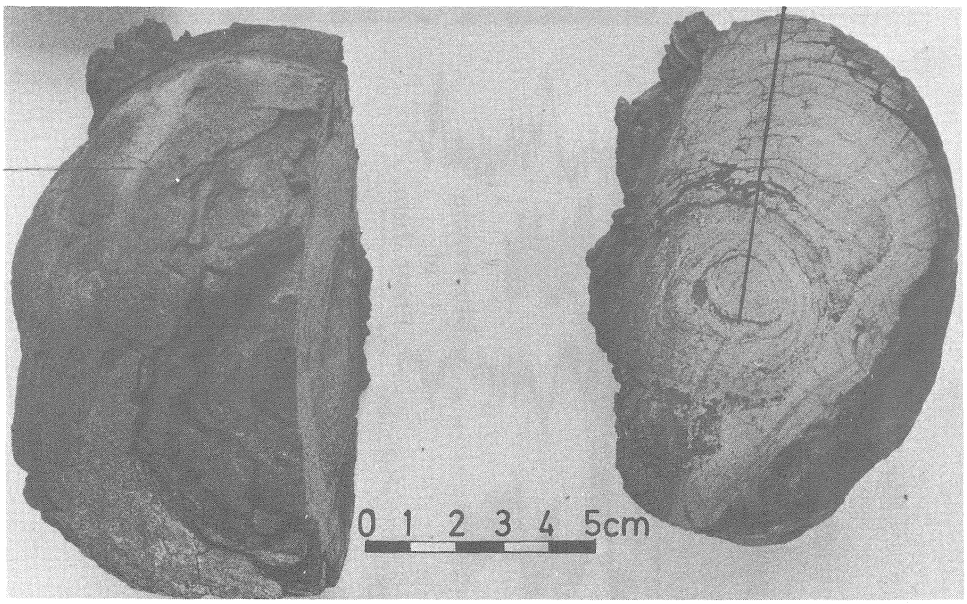

Plate I Photograph of the cut surface of the manganese nodule from the Suiko Seamount.

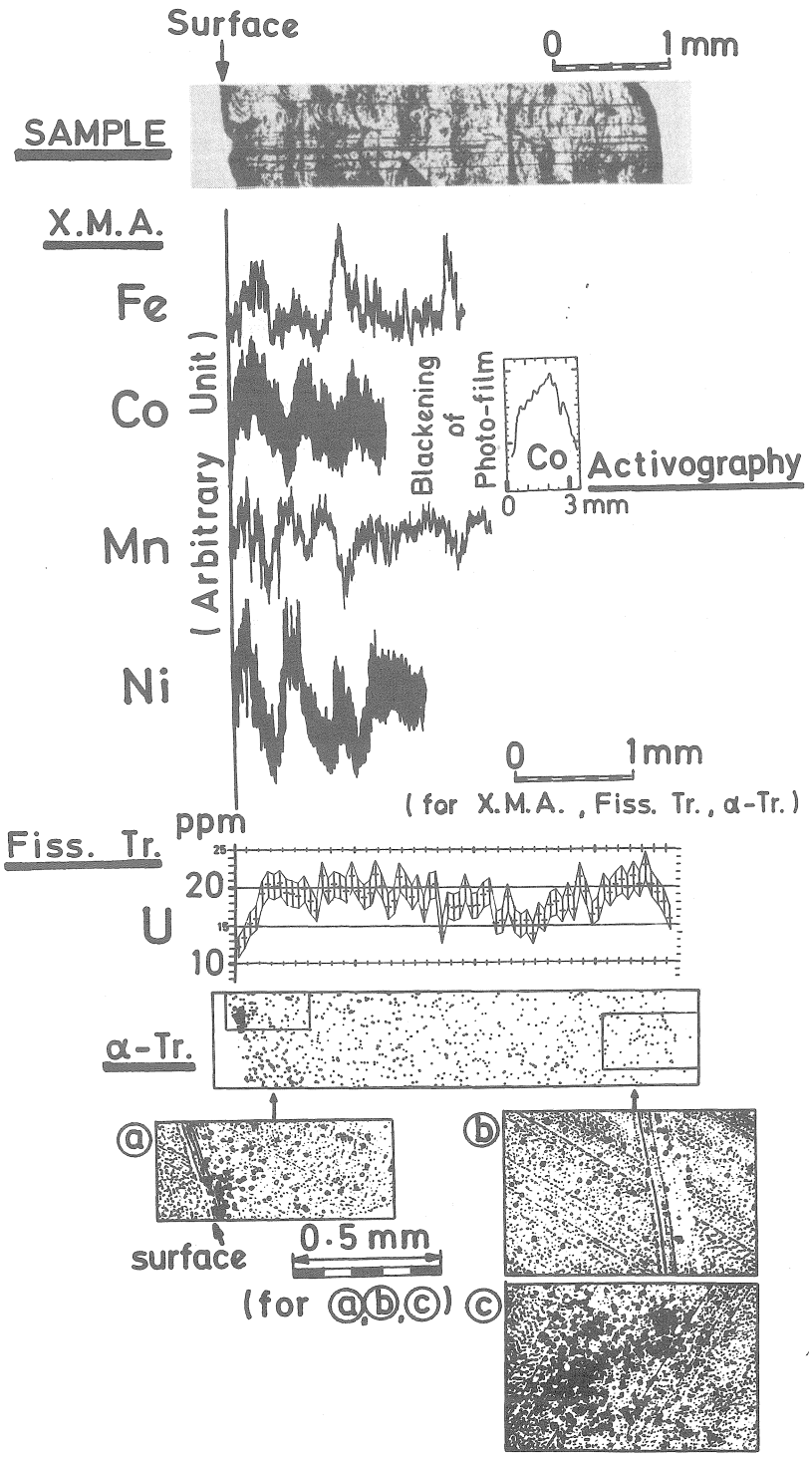

Plate II Distribution of iron, cobalt, manganese, nickel (determined by XMA), uranium (determined by fission track), and alpha radioactivity (observed by alpha track) in the crust of the Suiko manganese nodule. Cobalt distribution in an activograph (activation autoradiograph) was shown by the degree of blackening of photo-film as a function of depth. The top picture is the photomicrograph of polished cross section.

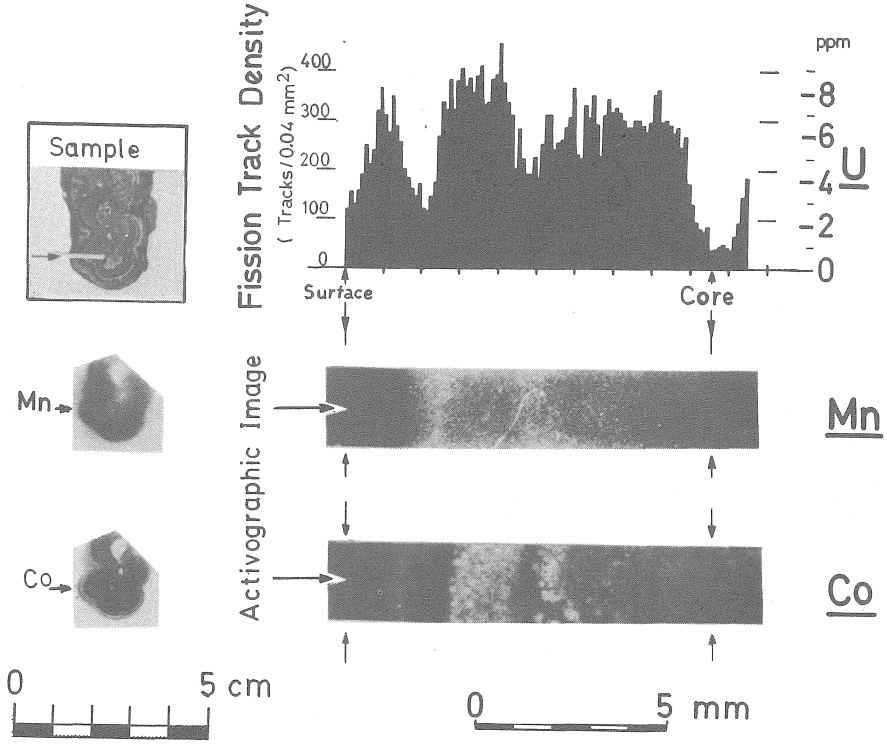

Plate III Distribution of uranium (determined by fission track), manganese and cobalt (observed by activograph) in the Central Equatorial Pacific manganese nodule. The black part of the activographic image shows the highly radioactive part (in the picture of the left side). The reverse tone of this image is shown at the right side picture (note the scale difference between the left and the right side).